J Mater Sci: Mater Med (2009) 20:223–228
DOI 10.1007/s10856-008-3563-6

XPS and biocompatibility studies of titania film on anodized NiTi shape memory alloy

C. L. Chu · R. M. Wang · T. Hu · L. H. Yin · Y. P. Pu · P. H. Lin · Y. S. Dong · C. Guo · C. Y. Chung · K. W. K. Yeung · Paul K. Chu

Received: 24 December 2007 / Accepted: 25 July 2008 / Published online: 30 August 2008

Abstract A dense titania film is fabricated in situ on NiTi shape memory alloy (SMA) by anodic oxidation in a Na_2SO_4 electrolyte. The microstructure of the titania film and its influence on the biocompatibility of NiTi SMA are investigated by scanning electron microscopy (SEM), X-ray photoelectron spectroscopy (XPS), inductively coupled plasma mass spectrometry (ICPMS), hemolysis analysis, and platelet adhesion test. The results indicate that the titania film has a Ni-free zone near the surface and can effectively block the release of harmful Ni ions from the NiTi substrate in simulated body fluids. Moreover, the wettability, hemolysis resistance, and thromboresistance of the NiTi sample are improved by this anodic oxidation method.

1 Introduction

NiTi shape memory alloys (SMA) are promising biomaterials because of their shape memory effect (SME) and super-elasticity (SE) [1, 2]. The high content of Ni (about 50 at%) in biomedical NiTi SMA is, however, of great health concern because release of Ni ions in the human body may cause allergic reactions and promote carcinogenesis and toxic reactions [3]. Moreover, in order to gain wider acceptance in cardiovascular products, it is imperative that the blood compatibility of NiTi SMA be improved in order to prevent thrombosis formation [4]. It has been shown that the biocompatibility can be improved by surface modification techniques such as plasma immersion ion implantation and deposition (PIII and D) [5] and biomimetic method with chemical pretreatment in alkali or H_2O_2 solutions [6] developed by Kokubo, Kim, van Blitterswijk, de Groot, and others [7, 8].

An artificial titania surface film can enhance the surface properties and reduce Ni out-diffusion from NiTi. Since NiTi SMA contains a large amount of Ti, it can be readily oxidized to form a surface titania film by thermal oxidation [9] or laser oxidation [10]. In our previous study, it was found that a titania film could be formed on NiTi SMA by Fenton's oxidation [11] which is a common way to remove inorganic and organic pollutants from water by oxidation of hydroxyl radicals (•OH) produced by catalysis decomposition of H_2O_2 with ferrous irons. Cheng et al. recently studied the microstructure of surface oxide films after anodic oxidation in a methanolic electrolyte or acetic acid as well as the corrosion behavior of anodized NiTi in Hank's solution [12, 13]. However, up to now, there have been very few systematic studies on the microstructure of titania films by anodic oxidation and their impact on the biocompatibility of NiTi including thromboresistance, hemolysis, leaching of harmful Ni ions, and wettability. In this work, a dense titania film was fabricated by anodic oxidation in a Na_2SO_4 electrolyte on the surface of NiTi SMA. The microstructure of the surface titania film and its influences on the biocompatibility

C. L. Chu (✉) · R. M. Wang · T. Hu · Y. S. Dong · C. Guo
School of Materials Science and Engineering and Jiangsu Key Laboratory for Advanced Metallic Materials, Southeast University, Nanjing 211189, China
e-mail: clchu@seu.edu.cn

L. H. Yin · Y. P. Pu
School of Public Health, Southeast University, Nanjing 210096, China

P. H. Lin
School of Materials Science and Engineering, Hohai University, Nanjing 210098, China

C. Y. Chung · K. W. K. Yeung · P. K. Chu
Department of Physics and Materials Science, City University of Hong Kong, Tat Chee Avenue, Kowloon, Hong Kong, China

of the NiTi SMA were investigated by scanning electron microscopy (SEM), X-ray photoelectron spectroscopy (XPS), inductively coupled plasma mass spectrometry (ICPMS), hemolysis analysis, and platelet adhesion test.

2 Experimental details

2.1 Fabrication of titania film on NiTi SMA by anodic oxidation

A biomedical NiTi (50.8 at% Ni) SMA plate was cut into small rectangular blocks 10 mm × 10 mm × 1 mm in size. The samples were chemically polished using a solution containing 5:1:4 of H_2O:HF:HNO_3 and ultrasonically washed in acetone and then deionized water for 10 min each. They were then divided into two groups. The first group was used as the control. The second group was treated by anodic oxidation at a constant current of 0.3 A for 60 min in an electrolytic cell consisting of a graphite cathode. The electrolyte was a 0.02 mol/l Na_2SO_4 aqueous solution at pH = 3.0.

2.2 Microstructure characterization

The surface morphology was observed by a Philips XL30 FEG SEM at 20 kV after the surface was coated with a thin layer of gold. The samples were analyzed by XPS on a VG Scientific ESCALAB 5 spectrometer with monochromatic Al K_α (1486.6 eV) X-ray radiation. The base pressure in the analysis chamber was better than 10^{-8} mbar. High-resolution Ti 2p, O 1s, and Ni 2p spectra were acquired at a 20 eV pass energy to determine the chemical states and concentrations. The XPS depth profiles were obtained by using a rastered 3 keV Ar^+ ion beam. The argon pressure during depth profiling was about 10^{-5} Pa and the sputtering rate was estimated to be 20 nm/min.

2.3 Biomedical properties

2.3.1 Ni release test

Two samples were immersed in 25 ml SBF in the same polypropylene bottle. The bottles were closed tightly and incubated in a thermostatic chamber at 37 ± 0.1°C for 2 and 5 weeks respectively. At each time point for each group, the SBF was taken out and analyzed by ICPMS to determine the amount of Ni leached from four specimens in two bottles.

2.3.2 Hemolysis and water contact angle

The contact angle was determined by averaging 10 measurements using the liquid drop method conducted on a contact angle goniometer (JC2000B, China). In the hemolysis test, 8 ml of fresh blood was collected from a rabbit and diluted with 10 ml 0.9% saline. Each sample was put into a test tube with 10 ml saline and incubated at 37°C for 30 min. Afterwards, 0.2 ml of the diluted blood was added to each test tube and incubation continued for another 60 min. After incubation, the suspension was centrifuged at 2,500 r/min for 5 min. The absorbance of the supernatant fluid was measured by a spectrophotometer (UV240, China). The positive control was a mixture of blood and deionized water and the negative control was a mixture of blood and saline. The hemolysis results were averages of three measurements.

2.3.3 Blood platelet adhesion

The samples were put into a 24-well tissue culture plate. A 3.8 wt% citrate acid solution was added to the blood with a blood to citrate acid ratio of 9:1. The solution was centrifuged to form a platelet-rich plasma (PRP) and erythrocyte. About 0.1 ml of the PRP was added to each well. After incubation at 37°C for 3 h, the PRP was taken from the wells. A phosphate buffer solution (PBS) was added to the wells and gently rinsed 2–3 times to get rid of the platelets adsorbed loosely on the sample surface. The samples were then soaked in 2.5% glutaraldehyde at room temperature for 12 h to fix the adhered platelets. The samples were subsequently dehydrated in 50%, 75%, 90%, and 100% ethanol for 10 min sequentially. After dehydration, the residual alcohol on the samples was cleaned off in 50%, 75%, 90%, and 100% isoamyl acetate aqueous solutions for 10 min. After critical point drying, the samples were coated with thin gold films and the distribution and morphology of the platelets were observed by SEM.

3 Results and discussion

3.1 Microstructure of titania film on anodized NiTi SMA

Figure 1 depicts the SEM photographs of the surfaces of the chemically polished and anodized NiTi SMA samples. The former is relatively smooth and the white particle-shape phase appearing in the parent phase is Ti_2Ni, which is confirmed by energy-dispersive X-ray analysis (EDS) performed in conjunction with SEM. In contrast, that a dense oxide film is formed on the NiTi SMA after anodic oxidation in the Na_2SO_4 electrolyte.

Figure 2 shows typical XPS survey spectra of the surfaces of the NiTi SMAs. The dominant elements are Ni, Ti, O, C on the chemically polished sample and Ti, O, C on the anodized one. The surface Ni concentration on the

chemically polished sample can reach as high as 11.4 at%, but there is no detectable Ni on the surface of the anodized sample. The results suggest that the anodized sample is covered by a dense titanium oxide film that has no detectable Ni. The presence of C may be attributed to surface contamination by carbon-containing molecules absorbed from the environment.

High-resolution XPS spectra taken to investigate the Ti and Ni binding energies in the near surface of the anodized one are displayed in Fig. 3. The Ti 2p XPS spectrum exhibits two dominant peaks that can be identified as Ti^{4+} (TiO_2) $2p_{3/2}$ at 458.8 eV and Ti^{4+} (TiO_2) $2p_{1/2}$ at 464.6 eV. No remnants of Ti^{Ni-Ti} in the intermetallic NiTi state can be found. In contrast, no Ni in any chemical states can be seen in the Ni 2p XPS spectrum further confirming the absence of Ni in the near surface of the anodized sample. The high-resolution O 1s XPS spectrum acquired from the near surface of the anodized one is shown in Fig. 4 together with the fitting curves. The dominant peak is also at 530.5 eV that can be assigned to oxygen in metal oxides. Other oxygen states such as adsorbed water and Ti–OH can also be detected.

The XPS depth profiles of Ni, Ti, and O are shown in Fig. 5. The oxygen profile shows a peak close to the top surface whereas the Ti profile shows a minimum concentration, which may be due to surface contamination from the cleaning solvents. The Ni concentration on the outermost surface is below the XPS detection limit. Afterwards, the O concentration decreases and the Ni concentration increases to a steady-state value of about 50 at% after 7 min sputtering. If the oxide thickness is estimated by taking the depth where the O signal drops to 50% of the maximum value, the thickness of the titania film on the anodized NiTi SMA is about 100 nm.

Figure 6 depicts the overlay of the high-resolution XPS Ni binding energy spectra of the anodized NiTi SMA at different sputtering time. Ni cannot be detected on the outermost surface. However, after sputtering for 3 min, two peaks with binding energies of about 853.8 and 870.5 eV associated with Ni^{Ni-Ti} $2p_{3/2}$ and $2p_{1/2}$ in the intermetallic NiTi state are detected. No Ni oxide peak can be found.

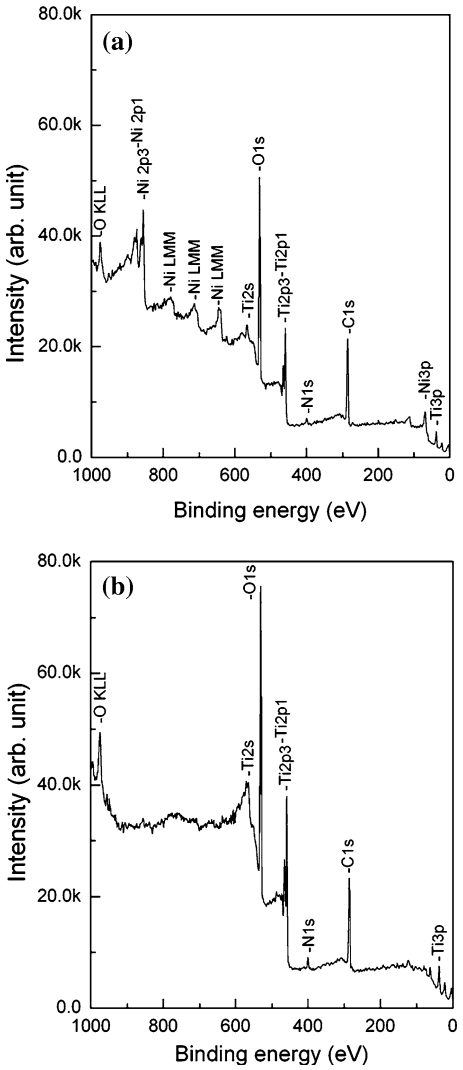

Fig. 2 XPS survey spectra of the surface of NiTi SMAs: (**a**) Chemically polished and (**b**) anodized

These two major peaks are unchanged with longer sputtering time. It should be pointed out that the Ni^{Ni-Ti} 2p spectra show an evident satellite structure which is separated from the main peaks by ~7 eV as shown in Fig. 6.

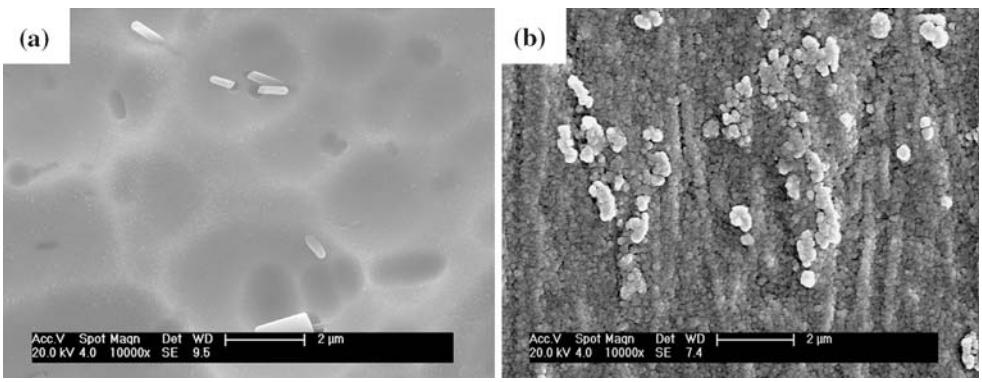

Fig. 1 Surface morphology of NiTi SMAs: (**a**) Chemically polished and (**b**) anodized

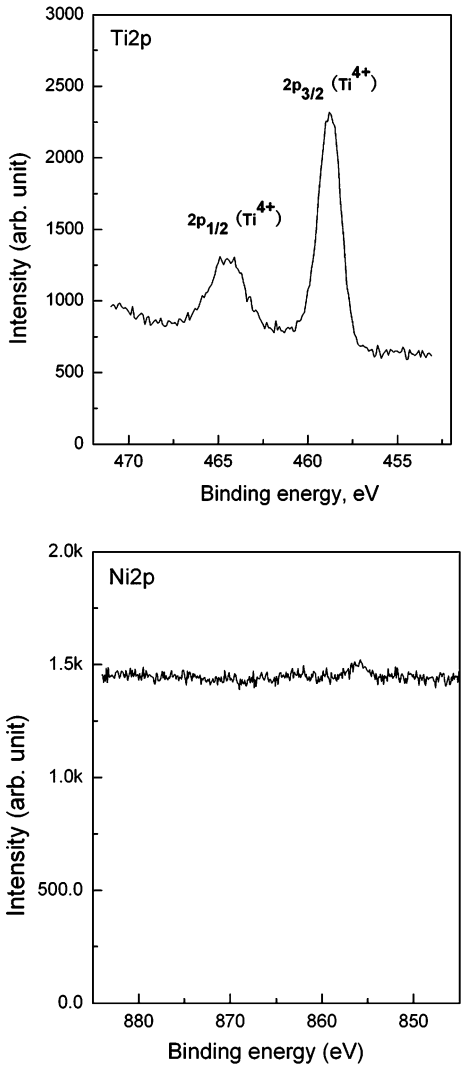

Fig. 3 Ti 2p and Ni 2p high-resolution XPS spectra of the surface on anodized NiTi SMA

The high-resolution XPS spectra in Fig. 7 show the changes in the Ti binding energy in the anodized NiTi SMA after different sputtering time. The XPS spectrum (curve (a) in Fig. 7) exhibits two dominant peaks that correspond to Ti^{4+} (TiO_2) $2p_{3/2}$ at 458.8 eV and Ti^{4+} (TiO_2) $2p_{1/2}$ at 464.6 eV. After 3 min sputtering, two small shoulders near 454.5 and 460.5 eV corresponding to the binding energies of Ti^{Ni-Ti} $2p_{3/2}$ and $2p_{1/2}$ spin states emerge and then change gradually into the dominant peaks as shown by curves (c)–(d) in Fig. 7. It indicates that Ti^{Ni-Ti} in the intermetallic NiTi state becomes the dominant Ti chemical state.

SEM and XPS results obviously reveal that a dense titania film composed of mainly TiO_2 phase is formed by anodic oxidation in a Na_2SO_4 electrolyte. The enrichment of Ti–OH groups on the surface of the titania film is expected because of the aqueous treatment. The existence of a Ni free zone on the surface can improve the biocompatibility of the NiTi SMA.

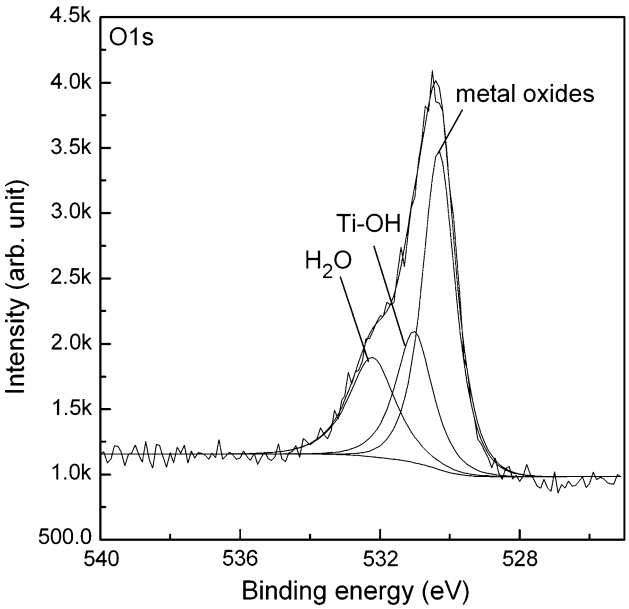

Fig. 4 O 1s high-resolution XPS spectra of the surface on anodized NiTi SMA

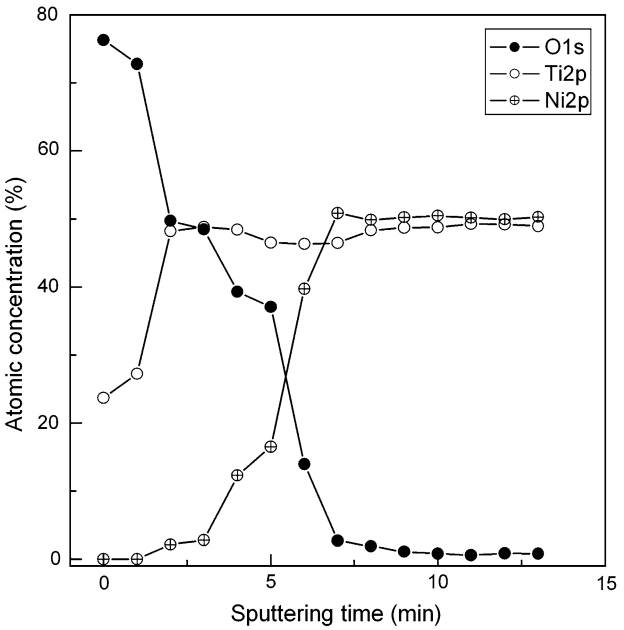

Fig. 5 XPS depth profiles showing the compositional changes in anodized NiTi SMA

3.2 Effects of titania film on biocompatibility of anodized NiTi SMA

Table 1 summarizes the ICPMS results after SBF immersion. The surface titania film on the anodized NiTi SMA can significantly reduce Ni release from the NiTi substrate. For the two immersion times (2 and 5 weeks), the amounts of Ni leached from the anodized NiTi are less than 5% of those leached from the chemically polished one.

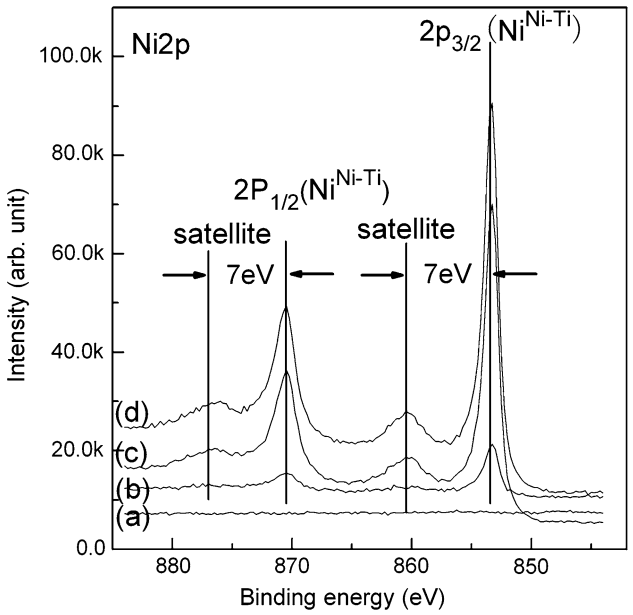

Fig. 6 Ni 2p XPS spectra of the surfaces of anodized NiTi SMA after different sputtering time: (**a**) 0 min, (**b**) 3 min, (**c**) 6 min, (**d**) 9 min

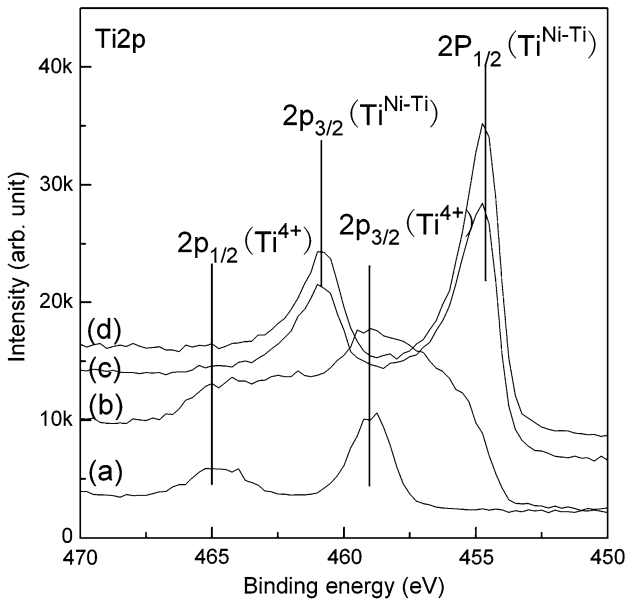

Fig. 7 Ti 2p XPS spectra of the surfaces of the anodized NiTi SMA after different sputtering time: (**a**) 0 min, (**b**) 3 min, (**c**) 6 min, (**d**) 9 min

Table 1 Concentrations (ppb) of Ni ions in SBF at 37 ± 0.5°C determined by ICPMS leached from NiTi SMAs for different immersion times (ppb)

Immersion times	2 weeks	5 weeks
The chemically polished one	314.6 ± 11.6	715.6 ± 13.4
The anodized one	6.1 ± 2.3	30.0 ± 5.2

Table 2 Hemolysis and water contact angles of NiTi SMAs

NiTi SMA	Hemolysis ratio (%)	Water contact angle (°)
The chemically polished one	4.26 ± 0.02	65.5° ± 5.8
The anodized one	2.61 ± 0.15	49.4° ± 4.6

Obviously, the titania film formed by anodic oxidation can mitigate out-diffusion of Ni from the substrate.

Table 2 lists the hemolysis ratios and water contact angles of the NiTi SMAs. The hemolytic activity is assessed by determining the hemoglobin release under static conditions. The hemolysis ratios determined from the chemically polished NiTi and anodized NiTi are less than 5%. The data suggest that both samples can meet the requirements for biomedical implants. However, a lower hemolysis ratio (2.61%) means that less hemolysis occurs on the surface of the anodized one. The contact angle of the chemically polished NiTi SMA is 65.5°, whereas that of the anodized one decreases to 49.4° due to the formation of titania film enriched with Ti–OH groups. Our results show that the wettability and hemolysis resistance of NiTi can be improved by the formation of a titania film using anodic oxidation.

The morphology of the adhered blood platelets on the NiTi SMAs after 3 h of incubation is shown in Fig. 8. The number of adherent platelets on the anodized NiTi is much less than that on the chemically polished one. Accumulation and pseudopodium of platelets are also serious on the chemically polished one as indicated by the three-dimensional structures connected by pseudopodium in Fig. 8a. In contrast, the platelets on the anodized sample form a single layer and are isolated (Fig. 8b). There is no sign of accumulation and only slight pseudopodium can be observed. Hence, platelet adhesion is reduced remarkably on the NiTi SMA after anodic oxidation and the thromboresistance of NiTi SMA can also be improved by fabrication of titania film. This may be related to the intrinsic electrical characteristics of titania film [14]. The formation of thrombus on an artificial material is correlated with charge transfer from the inactive state of fibrinogen to the materials surface [4]. Titania as a semiconducting material has a wide energy band gap of about 3.2 eV [15]. Fibrinogen also has an electronic structure similar to a semiconductor, but having a smaller band gap of 1.8 eV. The conduction and valence bands thus fall inside the energy gap of titania [16]. Hence, based on this argument, it is difficult for charges to be transferred from the valence band of fibrinogen to the titania and consequently, this may be one of the reasons why thrombus formation is inhibited. In addition, improvement in the wettability may also prevent adsorption of platelets and decrease platelet–surface interactions

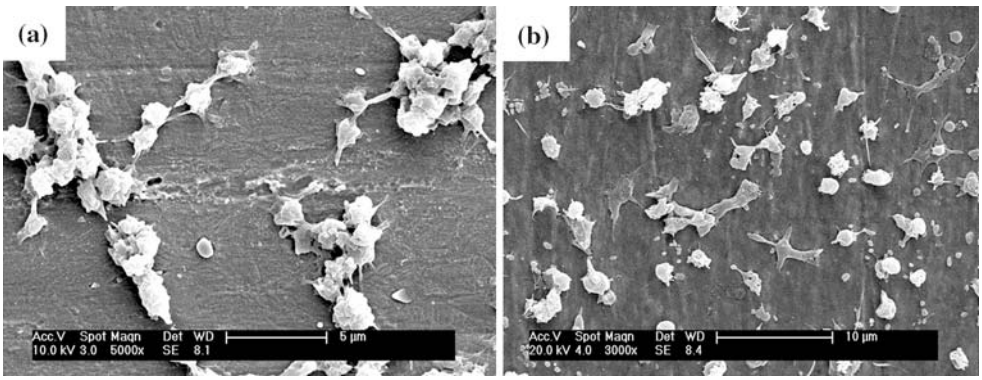

Fig. 8 SEM morphology of adherent platelets on the surface of NiTi SMAs after 180 min incubation in PRP: (**a**) Chemically polished and (**b**) anodized

[17]. In this study, the contact angle of the anodized NiTi SMA is found to be 49.4° which is smaller than that of the chemically polished one (65.5°) and believed to play an important role in the improved blood compatibility.

4 Conclusions

A dense titania film with a Ni-free surface zone has been synthesized in situ on biomedical NiTi SMA by anodic oxidation in a Na_2SO_4 electrolyte. The titania film effectively mitigates out-diffusion of Ni from the NiTi substrate when immersed in simulated body fluids. Moreover, the wettability, hemolysis resistance, and thromboresistance are much improved after anodic oxidation.

Acknowledgments The work described in this article was supported by Program for New Century Excellent Talents (NCET-06-0464) in University of Ministry of Education of China, National Natural Science Foundation of China (Project No.: 50501007), Natural Science Foundation of Jiangsu Province (Project No.: BK2007515), National High-tech Program-863 Projects of China (Project No.: 2006AA03Z445), Nippon Sheet Glass Foundation for Materials Science and Engineering (NSG Foundation), City University of Hong Kong Strategic Research Grant (SRG) No. 7001999, Hong Kong Research Grants Council (RGC), Central Allocation Grant No. 8730021.

References

1. T. Duerig, A. Pelton, D. Stockel, Mater. Sci. Eng. A **149**, 273–275 (1999). doi:10.1016/S0921-5093(99)00294-4
2. K. Otsuka, C.M. Wayman, *Shape Memory Materials* (Cambridge University Press, Cambridge, 1998)
3. D.F. Williams, in *Toxicology of Implanted Metals. Fundamental Aspects of Biocompatibility*. CRC Series in Biocompatibility, vol II (CRC Press, Boca Raton, FL, 1981), p. 45
4. R.E. Baier, R.C. Dutton, J. Biomed. Mater. Res. **3**, 191 (1969). doi:10.1002/jbm.820030115
5. R.W.Y. Poon, K.W.K. Yeung, X.Y. Liu, P.K. Chu, C.Y. Chung, W.W. Lu et al., Biomaterials **26**, 2265 (2005). doi:10.1016/j.biomaterials.2004.07.056
6. J. Choi, D. Bogdanski, M. Köller, S.A. Esenwein, D. Müller, G. Muhr, M. Epple, Biomaterials **24**, 3689 (2003). doi:10.1016/S0142-9612(03)00241-2
7. T. Kokubo, F. Miyaji, H.M. Kim, T. Nakamura, J. Am. Ceram. Soc. **79**, 1127 (1996). doi:10.1111/j.1151-2916.1996.tb08561.x
8. P. Habibovic, F. Barrĕre, C.A. Van Blitterswijk, K. De Groot, P. Layrolle, J. Am. Ceram. Soc. **85**, 517 (2002)
9. C.L. Chu, S.K. Wu, Y.C. Yen, Mater. Sci. Eng. A **216**, 193 (1996). doi:10.1016/0921-5093(96)10409-3
10. M.H. Wong, F.T. Cheng, H.C. Man, Mater. Lett. **61**, 3391 (2007). doi:10.1016/j.matlet.2006.11.081
11. C.L. Chu, T. Hu, S.L. Wu, Y.S. Dong, L.H. Yin, Y.P. Pu et al., Acta Biomater. **3**, 795 (2007). doi:10.1016/j.actbio.2007.03.002
12. F.T. Cheng, P. Shi, H.C. Man, Mater. Lett. **59**, 1516 (2005). doi:10.1016/j.matlet.2005.01.013
13. F.T. Cheng, P. Shi, G.K.H. Pang, M.H. Wong, H.C. Man, J. Alloy Comp. **438**, 238 (2007). doi:10.1016/j.jallcom.2006.08.020
14. N. Huang, P. Yang, X. Cheng, Y.X. Leng, X.L. Zheng, G.J. Cai et al., Biomaterials **19**, 771 (1998). doi:10.1016/S0142-9612(98)00212-9
15. R. Ebert, M. Schaldach, in *Ceramic As Material for Cardiovascular Device*. World Congress on Medical Physics and Biomedical Engineering, Hamburg, 1982
16. F. Gutmann, H. Keyzer, *Modern Bioelectrochemistry* (Plenum Press, New York, 1986)
17. F. Zhang, N. Huang, P. Yang, X.L. Zeng, Y.J. Mao, Z.H. Zheng et al., Surf. Coat. Tech. **84**, 476 (1996). doi:10.1016/S0257-8972(96)02848-4